

Thermally activated defects in float zone silicon: Effect of nitrogen on the introduction of deep level states

Jack Mullins,¹ Vladimir P. Markevich,¹ Michelle Vaqueiro-Contreras,¹ Nicholas E. Grant,² Leif Jensen,³ Jarosław Jabłoński,⁴ John D. Murphy,² Matthew P. Halsall,¹ and Anthony R. Peaker¹

¹Photon Science Institute and School of Electrical and Electronic Engineering, University of Manchester, Manchester M13 9PL, United Kingdom

²School of Engineering, University of Warwick, Coventry CV4 7AL, United Kingdom

³Topsil GlobalWafers A/S, Siliciumvej 1, DK-3600 Frederikssund, Denmark

⁴Topsil Semiconductors Sp. z o.o., 133 Wólczyńska St., 01-919 Warszawa, Poland

(Received 18 April 2018; accepted 27 June 2018; published online 16 July 2018)

Float zone silicon (FZ-Si) is typically assumed to be an extremely high quality material, with high minority carrier lifetimes and low concentrations of recombination active defects. However, minority carrier lifetime in FZ-Si has previously been shown to be unstable following thermal treatments between 450 and 700 °C, with a range of unidentified deep level states being linked to reduced carrier lifetime. There are suspicions that nitrogen doping, which occurs from the growth atmosphere, and intrinsic point defects play a role in the degradation. This study aims to address this by using deep level transient spectroscopy (DLTS), minority carrier transient spectroscopy, Laplace DLTS, and photoluminescence lifetime measurements to study recombination active defects in nitrogen-doped and nitrogen-lean n-type FZ-Si samples. We find that nitrogen-doped samples experience increased degradation due to higher concentrations of deep level defects during thermal treatments compared to nitrogen-lean samples. In an attempt to explain this difference, in-diffusion of nickel has been used as a marker to demonstrate the existence of higher vacancy concentrations in the nitrogen-doped samples. The origin of the recombination active defects responsible for the thermally induced lifetime degradation in FZ-Si crystals is discussed. © 2018 Author(s). All article content, except where otherwise noted, is licensed under a Creative Commons Attribution (CC BY) license (<http://creativecommons.org/licenses/by/4.0/>). <https://doi.org/10.1063/1.5036718>

I. INTRODUCTION

Float zone (FZ) growth of silicon allows the production of high purity wafers, with significantly lower concentrations of impurities than in Si grown by directional solidification methods, and crucially, lower concentrations of light impurities, such as oxygen and carbon, than those found in silicon grown using the Czochralski (Cz) technique.¹ Low oxygen concentrations (typically below 10^{16} cm^{-3}) are achieved by the FZ process because the silicon melt is not in contact with a quartz crucible, which in the case of Cz-Si results in oxygen concentrations of the order 10^{18} cm^{-3} .² Silicon wafers grown by the float zone method often have high minority carrier lifetime and better doping uniformity than the Cz material. They are used in power devices where a closely controlled lifetime is required and for the production of the highest efficiency solar cells where very high lifetime is a prerequisite. They are also used as reference samples for the development of new surface passivation processes and in the development of extremely high efficiency laboratory solar cells.

However, recent studies^{3–6} have shown that the minority carrier lifetime in some FZ-Si wafers is not stable and can be reduced by a factor of more than 100 following thermal treatment in the temperature range of 450–700 °C. The observed reduction in carrier lifetime has been linked to the introduction of a number of deep level defects upon annealing but to date no clear identification of these defects has

been possible. The minority carrier lifetime reduction following annealing is most significant in vacancy-rich regions of the FZ-Si wafers studied,⁴ suggesting that vacancies play a role in the process of defect formation, and light impurities, including nitrogen,⁷ have also been suggested to influence the reduction in carrier lifetime, possibly in complexes with vacancies. It should be also noted that recent studies have found bulk lifetime degradation in FZ-Si wafers upon typical solar cell operation conditions (so-called light induced degradation),^{8,9} and the origin of this effect could be related to the thermal instability found previously.

Growth ambient atmospheres containing nitrogen are typically used by float zone silicon manufacturers^{10,11} in order to incorporate nitrogen into the silicon melt during crystal growth, as it has been found to result in significant improvements of the finished wafers. Most importantly, nitrogen doping is found to increase crystal strength^{12,13} as well as to prevent the agglomeration of silicon vacancies into voids¹⁴ and enhance the annihilation of vacancies with Si self-interstitial atoms during crystal growth.^{10,15} Nitrogen added to silicon during growth is found to be present mainly as an electrically inactive di-interstitial,¹⁶ N_2 , and as such has no or little direct impact on the recombination activity in nitrogen doped wafers. Although there is evidence for the formation of electrically active nitrogen-oxygen complexes in Si,^{15,17,18} these are seen to occur in nitrogen doped

Czochralski (Cz) silicon samples with reasonably high oxygen concentrations. Theoretical work has suggested that minority nitrogen species other than the interstitial dimer may have defect states within the bandgap of silicon.¹⁹

In this work, we have investigated the role of nitrogen doping in the formation of thermally activated deep level defects in FZ-Si using photoluminescence (PL) carrier lifetime measurements as well as deep level transient spectroscopy (DLTS), high resolution Laplace DLTS (L-DLTS),²⁰ and minority carrier transient spectroscopy (MCTS).²¹ To study the vacancy concentrations in the material, we have performed experiments based on vacancy decoration by metal atoms. This is an established method of measuring low concentrations of vacancies in silicon crystals^{22–24} in which in-diffused interstitial metal atoms interact with existing vacancy-related defects and occupy substitutional sites.

If the substitutional metal atoms are electrically active and positions of their energy levels are known, concentrations of these defects can be measured using DLTS and give an indication of the vacancy concentration within the wafer.^{22–24} In this study, nickel was used and substitutional nickel atoms are known to introduce two acceptor energy levels in n-type silicon, $E(-/-)$ and $E(-/0)$ at about 0.07 eV and 0.42 ± 0.04 eV from the conduction band edge, respectively.^{25,26}

II. EXPERIMENTAL METHODS

Two sets of 100 mm diameter $\langle 100 \rangle$ phosphorous doped n-type FZ-Si wafers, with resistivity 1–5 Ω cm, were studied in this work; nitrogen rich (with thickness ~ 280 μ m and $[N] \sim 6 \times 10^{14}$ cm⁻³) and nitrogen lean (with thickness ~ 500 μ m and $[N] < 2 \times 10^{14}$ cm⁻³, below the detection limit of secondary ion mass spectroscopy). The materials were grown by the same manufacturer with identical growth conditions with the exception of the ambient atmosphere. Quarters of these wafers were subjected to the RCA cleaning and then to heat-treatments in different gas ambient atmospheres (oxygen, argon, and nitrogen) for 30 min at temperatures in the range of 450–700 °C in order to introduce lifetime limiting defects, as well as at high temperature (≥ 950 °C) at which they have been previously shown to become permanently deactivated.^{3–6} In order to establish the possible role of vacancies, nickel was intentionally in-diffused into samples of nitrogen rich and nitrogen lean float zone silicon. Nickel was thermally evaporated onto the surface of the samples, which were then annealed at 500 °C for 90 min in order to in-diffuse interstitial nickel atoms which after interactions with Si vacancies available in the bulk become observable in DLTS measurements.^{22,27,28} Samples of the same material but with no nickel contamination were subjected to the same annealing treatment to act as a control.

Photoluminescence (PL) imaging carrier lifetime measurements²⁹ were undertaken before and after heat treatments, using a superacid-based surface passivation technique described in Refs. 30 and 31 with a BT Imaging LIS-L1 system. The superacid-based passivation technique provides excellent surface recombination velocities (around 1 cm/s for this doping and type³⁰) whilst being a room temperature

technique. The use of this technique allows us to avoid possible defect reactions and associated lifetime changes that can occur upon the use of more conventional dielectric-based surface passivation schemes requiring treatments at 200 to 400 °C. Using PL lifetime images for the identification of defect-rich regions, samples were cut from appropriate locations of as-grown and annealed wafers for measurement by DLTS and MCTS.

Circular Schottky barrier diodes (SBDs) of diameter 1 mm were formed on the surface of the samples using thermal evaporation of Au through a shadow mask, while a layer of Al was thermally evaporated onto the back surface to create an Ohmic contact. For samples used in MCTS measurements, a small region of the back surface was covered during Al evaporation to leave a “window” of silicon to allow optical excitation using a 940 nm light emitting diode (LED). The diodes were characterized using capacitance-voltage (C-V) and current-voltage measurements, and the highest quality diodes were chosen for DLTS and MCTS measurement to study deep level defects.

For the vacancy decoration experiments, nickel (99.999% purity) was thermally evaporated onto the surface of nitrogen rich and nitrogen lean float zone silicon samples, and the samples were annealed at 500 °C for 90 min. The times and temperatures were chosen to ensure complete Ni diffusion through the wafers. Extrapolation of data from Lindroos *et al.*³² gives a diffusion coefficient (D) at 500 °C of 1.8×10^{-5} cm²s⁻¹ which corresponds to a \sqrt{Dt} diffusion length of 1.8 mm in the time (t) used, which is more than sufficient for Ni to penetrate the whole sample. After contamination, both sets of samples were etched in a mixture of 1HF:7HNO₃ for 3 minutes. Etching has resulted in the removal of the evaporated nickel and a silicon layer of ~ 40 μ m. The heat-treated samples were then prepared for electrical measurement as described previously.

III. RESULTS

A. Carrier lifetime measurements

Figure 1 shows calibrated photoluminescence minority carrier lifetime images recorded on nitrogen lean and nitrogen rich wafers in the as-grown state [(a) and (b)] and after annealing at 600 °C for 30 min in oxygen [(c) and (d)].

It can be seen in Fig. 1 that in the as-grown state for both wafers the carrier lifetime is fairly high (> 1 ms) and relatively uniform across the wafer. The effective lifetime measured in the nitrogen lean case is slightly higher than that in the nitrogen rich case. It is however noted that the wafers have substantially different thicknesses, so the impact of the remaining surface recombination on the measured lifetime is not the same in both cases. However, after annealing at a temperature seen in previous works^{3–6} to reduce minority carrier lifetime (600 °C), substantial differences between the lifetime images of the nitrogen rich and nitrogen lean samples have arisen.

Although in both cases carrier lifetime is seen to be reduced, the reduction is far more severe (over 100 times in the worst affected regions) in the nitrogen rich wafer, with a characteristic lifetime reduction in the wafer centre, seen

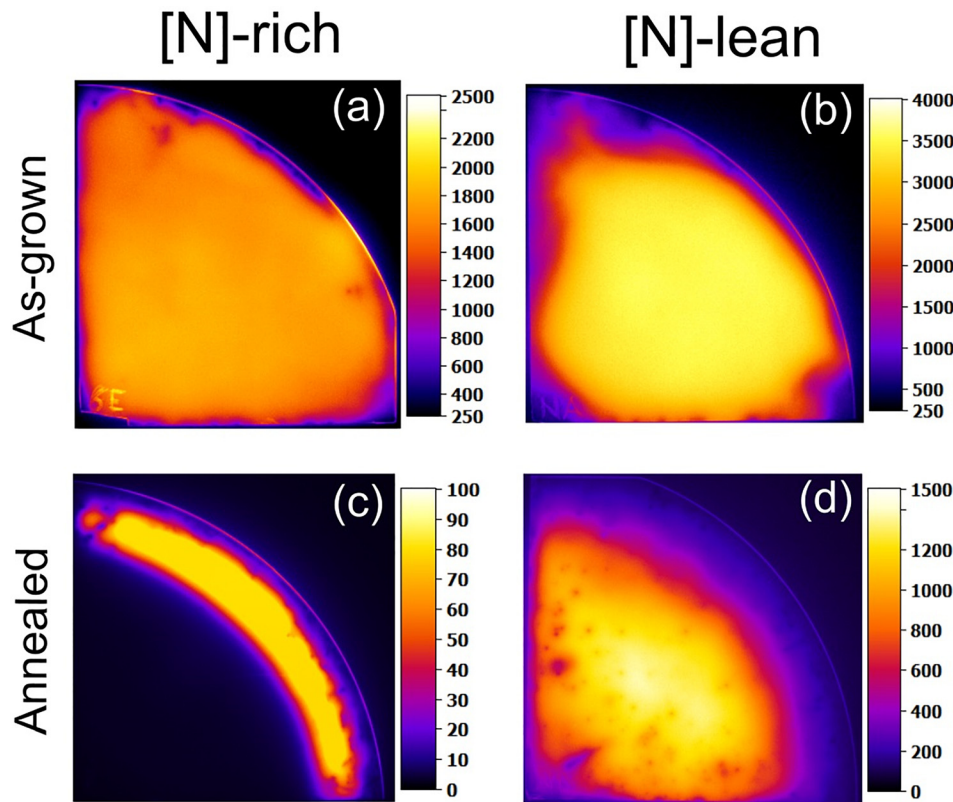


FIG. 1. Calibrated photoluminescence carrier lifetime images of 280 μm thick nitrogen rich [(a), (c)] and 500 μm thick nitrogen lean [(b), (d)] n-type float zone silicon quarter wafers in the as-grown state and following annealing at 600 $^{\circ}\text{C}$ for 30 min in O_2 . Minority carrier lifetime values are in microseconds. Sample radii are ~ 50 mm.

previously in Ref. 4 and a relatively high lifetime ring present around the wafer edge. This ring-like patterning has been suggested to be related to the radial distribution of vacancies within the wafer.⁴ It is known that the central region of FZ-Si wafers, which are cut from ingots grown with a relatively high growth rate (≥ 3.5 mm/min), is vacancy rich, while close to the wafer edges, a defect neutral or interstitial rich region is present.^{10,33}

The lifetime degradation is less pronounced in the nitrogen lean wafer, and the characteristic patterning seen in the nitrogen rich sample is not present, with the regions of lowest lifetime found to be located close to the wafer edge in this case, although the reason for this inversion is unclear. Crucially, Fig. 1 shows that the severity of thermally induced lifetime degradation of float zone silicon is much greater in the nitrogen rich case.

B. DLTS study of annealed N-rich and N-lean Si

To link the difference in lifetime degradation to the introduction of thermally activated defects, electrical measurements were carried out to identify the deep level electronic defects responsible and investigate if the differences in either the types of defects introduced or their concentration could be linked to the difference in nitrogen content in the samples. Figure 2 shows DLTS spectra recorded on samples of n-type nitrogen rich FZ-Si cut from the wafer center in the as-grown state and following annealing at 500 $^{\circ}\text{C}$, 950 $^{\circ}\text{C}$, and 950 $^{\circ}\text{C}$ followed by 500 $^{\circ}\text{C}$ for 30 min in Ar. Before any annealing treatment, the DLTS spectrum is flat, and no deep level electronic traps are seen to be present. This implies that the electron trap concentration is less than $5 \times 10^{11} \text{ cm}^{-3}$.

After annealing at 500 $^{\circ}\text{C}$, two strong peaks with their maxima at ~ 110 K and ~ 200 K, which are labelled as E_1 and E_2 , and a few minor signals are observed in the DLTS spectrum. The dominant peaks correspond to traps with activation energies for electron emission (ΔE_c) at 0.18 eV (E_1) and 0.34 eV (E_2) relative to the conduction band minimum and apparent capture cross sections, σ_{app} , $\sim 6 \times 10^{-17} \text{ cm}^2$ (E_1) and $7 \times 10^{-17} \text{ cm}^2$ (E_2) as determined from Arrhenius

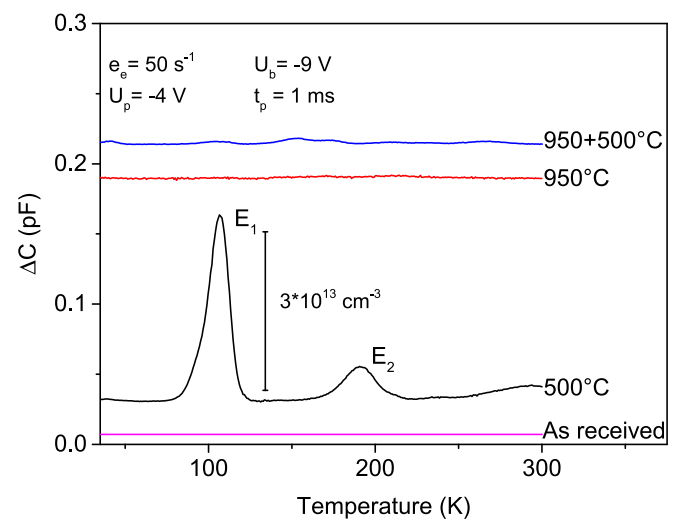


FIG. 2. DLTS spectra recorded on the samples from the central region of a n-type nitrogen rich FZ-Si wafer in the as received state, and following 30 min annealing in Ar at 500 $^{\circ}\text{C}$, 950 $^{\circ}\text{C}$, and 950 $^{\circ}\text{C}$ followed by 500 $^{\circ}\text{C}$. Measurement settings [DLTS rate window (e_0), bias voltage (U_b), filling pulse voltage (U_p), and filling pulse lengths (t_p)] and the defect concentration unit bar are shown in the graph. The spectra are shifted on the vertical axis for clarity.

plots of T^2 -corrected electron emission rates measured with the use of L-DLTS. The concentrations of the traps are $\sim 3 \times 10^{13} \text{ cm}^{-3}$ and $\sim 3 \times 10^{12} \text{ cm}^{-3}$. The true values of the capture cross sections, σ_t , of these defects have been determined using Laplace DLTS measurements with varying filling pulse widths between 60 ns and 20 ms to be $1.2 \times 10^{-17} \text{ cm}^2$ (E_1) and $1.7 \times 10^{-17} \text{ cm}^2$ (E_2). Neither of the capture cross sections were found to be temperature dependent. Typical dependencies of Laplace DLTS signal strength (ΔC) on filling pulse length (t_p) for the E_1 and E_2 traps are shown in Fig. 3. For both E_1 and E_2 traps, the Laplace DLTS signal saturates for long filling pulses, and the measured $\Delta C(t_p)$ dependencies can be satisfactorily described by the mono-exponential growth law. Such $\Delta C(t_p)$ dependencies are characteristic of point defects in contrast to extended defects like precipitates and dislocations for which logarithmic $\Delta C(t_p)$ dependencies are usually observed.^{34,35}

The measured characteristics of the most prominent defect level, E_1 , are similar to those ($\Delta E_c = 0.19 \text{ eV}$ and $\sigma_{\text{app}} = 8 \times 10^{-17} \text{ cm}^2$) for an electron trap observed in DLTS spectra of n-type FZ-Si Si crystals doped with nitrogen during growth.³⁶ The trap was not detected in samples from ingots grown under similar grown conditions but without nitrogen added to the melt.³⁶

The behaviour of the defect levels observed in the present work upon high temperature annealing is similar to the results reported in Ref. 4, according to which annealing at high temperatures ($>950^\circ\text{C}$) has not resulted in the introduction of defect levels, and furthermore, no comparable concentration of traps has been introduced upon annealing at 500°C following the high temperature annealing.

The results of corresponding measurements carried out on nitrogen lean silicon samples are shown in Fig. 4. In contrast to the nitrogen rich samples, the DLTS spectra recorded on nitrogen lean wafers show no significant concentrations of defects introduced upon annealing at 500°C as well as after heat-treatments at higher temperatures. As the lifetime of the nitrogen lean wafers was still seen to be reduced

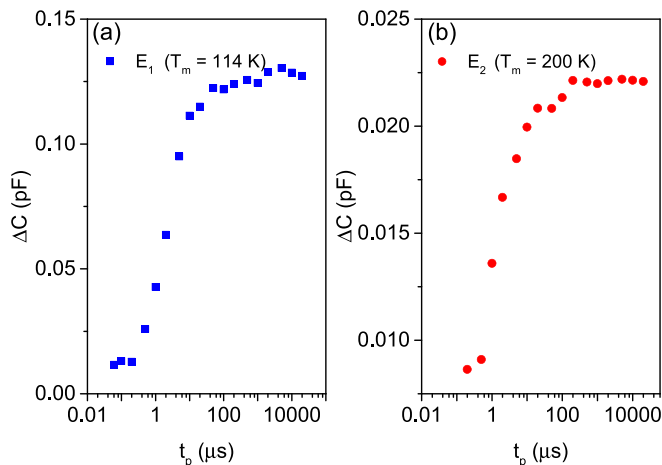


FIG. 3. Dependencies of Laplace DLTS peak amplitudes on the filling pulse length (t_p) at measurement temperatures (T_m) of 114 K and 200 K for the E_1 and E_2 traps, respectively, in nitrogen rich float zone silicon annealed in Ar for 30 min at 500°C . The dependencies obtained demonstrate that the traps are related to point-like defects.

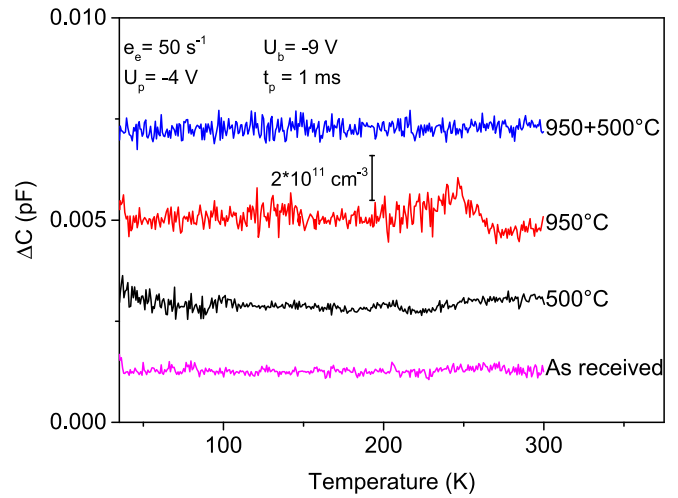


FIG. 4. DLTS spectra recorded on the samples from the central region of an n-type nitrogen lean FZ-Si wafer in the as grown state and following 30 min annealing in Ar at 500°C , 950°C , and 950°C followed by 500°C . Measurement settings and the defect concentration unit bar are shown in the graph. The spectra are shifted on the vertical axis for clarity.

following annealing (Fig. 1), it is suggested that a very low concentration of deep level electronic defects is introduced during annealing at 500°C , but that the concentration is below the detection limit of the DLTS equipment used in this study ($\sim 10^{11} \text{ cm}^{-3}$).

It has been suggested in Refs. 3–6 that the reduction of lifetime in FZ-Si wafers upon their annealing in the temperature range of 450 – 700°C occurs because of the formation of recombination centers in the bulk of the annealed wafers. However, depth distributions of the recombination active defects have not been studied carefully. Figure 5 shows concentration-depth profiles of the E_1 and E_2 traps in a FZ-Si sample annealed in an Ar ambient atmosphere. It appears that the spatial distribution of the traps introduced by the heat-treatment is uniform in the region probed by the DLTS profiling measurements, so indicating that the formation of the E_1 and E_2 traps occurs in bulk of the wafers upon annealing.

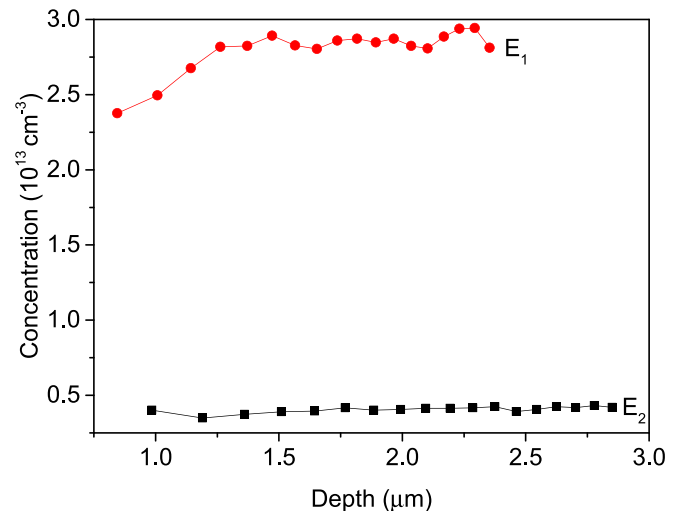


FIG. 5. Concentration-depth plots of the thermally activated E_1 and E_2 defects in a sample from n-type nitrogen rich float zone silicon which was annealed in Ar for 30 min at 500°C .

C. Effect of annealing ambient atmosphere

It is known that heat-treatments of Si samples in different gas ambient atmospheres can result in different chemical reactions on the Si surface and the introduction of different defects into the subsurface layers.³⁷ So, to obtain further information about the origin of the thermally activated recombination centers in FZ-Si wafers and their spatial distribution, we have studied the effect of the annealing ambient atmosphere on the introduction of deep level defects for both nitrogen rich and nitrogen lean silicon. Samples of each material were annealed at 500 °C for 30 min in Ar, N₂, and O₂, after which DLTS spectra were recorded. The results of these measurements are shown in Fig. 6.

The significant differences observed between the DLTS spectra recorded on annealed samples of nitrogen rich and nitrogen lean Si can be clearly seen in Fig. 6. In nitrogen lean silicon, no measurable concentration of defects is detected, regardless of the ambient atmosphere used, again suggesting that if defect states are introduced, their concentration is very low ($<10^{11} \text{ cm}^{-3}$). In nitrogen rich silicon, a significant concentration ($\sim 10^{13} \text{ cm}^{-3}$) of deep level defects is introduced upon annealing, with minimal differences seen between the DLTS spectra for samples annealed in different ambient atmospheres. Although some small variations in magnitudes of the dominant peaks are seen in the DLTS spectra, these most likely occur due to the lateral variation in defect concentration across the wafer and are not associated with the changes in the annealing ambient atmosphere. This result provides further evidence to support the hypothesis that the introduction of the E₁ and E₂ traps into N-rich FZ-Si wafers upon their annealing is related to defect reactions in the bulk and is not due to surface-related effects.

D. MCTS measurements

Minority carrier transient spectroscopy was used to investigate the introduction of traps in the lower half of the

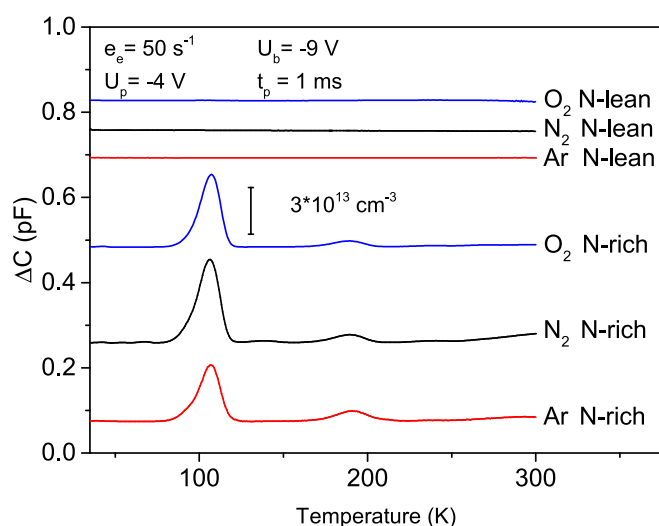


FIG. 6. DLTS spectra recorded on n-type nitrogen rich and nitrogen lean float zone silicon following annealing at 500 °C for 30 min in Ar, N₂, and O₂. Measurement settings and the defect concentration unit bar are shown in the graph. The spectra are shifted on the vertical axis for clarity.

silicon band gap on samples of both nitrogen rich and nitrogen lean wafers following annealing at 500 °C in Ar. The results of these measurements are shown in Fig. 7.

Similar to the DLTS spectra shown in Figs. 2, 4, and 6, there is a large difference between the MCTS spectra recorded on nitrogen rich and nitrogen lean silicon following annealing. In the nitrogen lean case, no clear peaks are observed, again suggesting that if any deep level traps are present, their concentration is extremely low. In the spectrum recorded from the nitrogen rich sample, three clear peaks are seen with their maxima at ~ 100 K, 210 K, and 270 K and labelled H₁, H₂, and H₃, respectively. Using Laplace MCTS measurements, the H₂ peak was found to be the result of hole emission signals from two separate electrically active levels, hence referred to as traps H_{2a} and H_{2b}.

The electronic characteristics of the H₁-H₃ traps were determined using Laplace MCTS. The activation energies of hole emission were determined from Arrhenius plots of T²-corrected hole emission rates as 0.22 eV (H₁), 0.48 eV (H_{2a}), 0.41 eV, (H_{2b}), and 0.71 eV (H₃) from the valence band maximum. Although the H₃ trap was found to have an activation energy for hole emission greater than half the bandgap, it is likely that there is an associated barrier for hole capture and that the true energy level position for this trap is closer to the valence band, as seen for traps with similar measured activation energies such as those in Ref. 38. Measurements of trap concentrations (N_T) using MCTS are more complicated and not as precise compared to those with the use of DLTS; however, low limits of N_T values can be derived from a combined analysis of C-V data and MCTS spectra.²¹ The low limit values of concentrations for the H₁-H₃ traps are given in Table I.

Using a value for the minority carrier concentration determined from the photo-current at the temperature of trap filling measurements, the capture cross sections for holes (minority carriers in this case), σ_p , have also been determined from Laplace MCTS measurements with varying LED pulse widths between 60 ns and 70 ms. The hole capture cross sections were calculated to be $1.2 \times 10^{-14} \text{ cm}^2$ (H₁), $3.1 \times 10^{-14} \text{ cm}^2$ (H_{2a}), $7.0 \times 10^{-13} \text{ cm}^2$ (H_{2b}), and $\geq 10^{-15}$

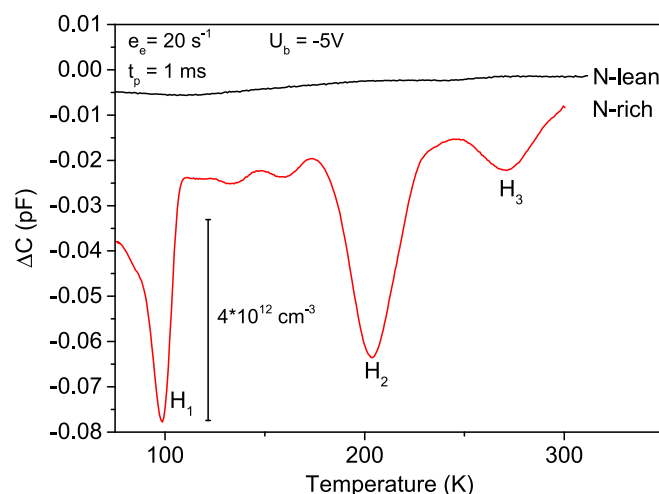


FIG. 7. MCTS spectra recorded on nitrogen rich and nitrogen lean n-type FZ-Si annealed at 500 °C for 30 min in Ar.

TABLE I. Properties of electrically active states measured in the samples from central parts of nitrogen rich silicon following annealing at 500 °C for 30 min.

Trap	ΔE (eV)	σ_n (cm ⁻²)	σ_p (cm ⁻²)	Average concentration (cm ⁻³)	Measured by
E ₁	E _c - 0.18	1.2×10^{-17}	Not measured	$\sim 3 \times 10^{13}$	L-DLTS
E ₂	E _c - 0.34	1.7×10^{-17}	Not measured	$\sim (2-4) \times 10^{12}$	L-DLTS
H ₁	E _v + 0.22	Not measured	1.2×10^{-14}	$> 4 \times 10^{12}$	L-MCTS
H _{2a}	E _v + 0.48	2.3×10^{-18}	3.1×10^{-14}	$> 3 \times 10^{12}$	L-MCTS
H _{2b}	E _v + 0.41	8.5×10^{-19}	7.0×10^{-13}	$> 3 \times 10^{12}$	L-MCTS
H ₃	E _v + 0.71	Not measured	$\geq 10^{-15}$	$> 1 \times 10^{12}$	L-MCTS

cm² (H₃). The hole capture cross sections measured were not found to be temperature dependent, except for the H₃ trap. We have attempted to measure temperature dependence of the hole capture cross section for the H₃ trap; however, the small signal strength has prevented an accurate analysis and the associated capture barrier has only been estimated to be > 0.1 eV.

The capture cross section for majority carriers has also been measured for the H_{2a} and H_{2b} traps through the use of a long optical “filling pulse,” followed by a zero bias “clearance pulse” which was varied in length. During the filling pulse, deep level traps are completely filled with holes and further are able to trap electrons when the clearance pulse is applied. Depending on the length of this clearance pulse, the measured signal due to hole emission can be reduced and this measured reduction with varying pulse length can be used to determine the majority carrier capture cross section of a given deep level trap. The electron capture cross sections for the H_{2a} and H_{2b} traps were found to be 2.3×10^{-18} cm² and 8.5×10^{-19} cm², respectively. Analysis of the ratio of the electron and hole capture cross sections for the H_{2a} and H_{2b} traps indicates that these traps are related to acceptor levels. Based on the capture cross section values and relative concentrations of the H₁-H₃ traps, it appears that the H_{2a} and H_{2b} traps are likely to be the dominant minority carrier recombination centers in this material.

E. Ni in-diffusion experiment—Evidence for the involvement of vacancies

Positron annihilation spectroscopy (PAS) is the standard technique for determining the concentration and nature of vacancy related defects in semiconductors. Unfortunately, the detectivity of the technique is not high and attempts of two groups to observe vacancy related defects in either the as grown or annealed samples of both nitrogen-rich and nitrogen-lean FZ-Si materials using state-of-the-art PAS equipment have not been successful. This is not unexpected as previous positron annihilation measurements have only been successful in cases where the vacancy concentration has been increased by either electron irradiation or ion implantation.³⁹ As a consequence, in order to establish whether any of the traps observed in DLTS measurements of annealed float zone silicon are due to defects incorporating vacancies, a series of DLTS measurements were carried out on samples of float zone silicon after vacancy decoration with fast diffusing metal atoms—in this case Ni.²²

The DLTS spectra for Ni-contaminated samples were compared with those for samples of the same materials with

no nickel at the surface subjected to the identical heat-treatment. DLTS spectra recorded on samples of nitrogen rich FZ silicon with and without evaporated nickel after annealing at 500 °C for 90 min are shown in Fig. 8. In samples with no evaporated nickel (spectra 2 and 4 in Fig. 8), DLTS peaks with their maxima at ~ 110 K and ~ 200 K are observed, which are similar to those described earlier in the paper as related to the E₁ and E₂ traps seen in nitrogen rich silicon annealed for 30 min at 500 °C in Fig. 2. It can be seen that in the sample cut from the wafer edge (spectrum 2), the magnitudes of the DLTS peaks are smaller than in the sample cut from the wafer center (spectrum 4), indicating a lower concentration of defects at wafer edges as expected from the lifetime measurements.

In the DLTS spectra of samples with evaporated nickel (spectra 1 and 3), two new peaks with their maxima at ~ 45 K and ~ 225 K have appeared with approximately equal magnitudes. The activation energies of electron emission have been determined for these traps to be 0.08 and 0.42 eV from the conduction band minimum, which are close to those for acceptor levels of substitutional Ni in Si.²² So, the traps have been assigned to the E(-/-) and E(-/0) levels of substitutional nickel, respectively.

From an analysis of the DLTS spectra presented in Fig. 8, some important information about defects in the nitrogen-rich FZ-Si material has been obtained. First, a comparison of

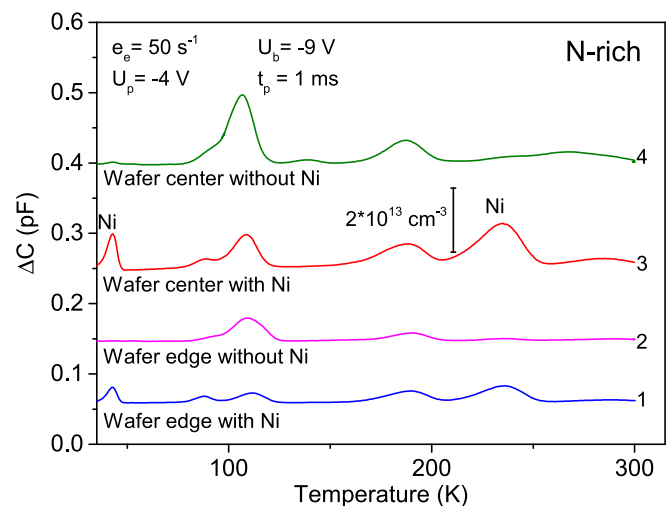


FIG. 8. DLTS spectra recorded on n-type nitrogen rich float zone silicon cut from the wafer edge (spectra 1 and 2) and center (spectra 3 and 4) with (spectra 1 and 3) and without (spectra 2 and 4) thermal evaporation of nickel, following annealing at 500 °C for 90 min in N₂. Measurement settings and the defect concentration unit bar are shown in the graph. The spectra are shifted on the vertical axis for clarity.

the spectra 1 and 3 indicates that the concentration of substitutional nickel, and hence the implied vacancy concentration, is higher in the sample cut from the wafer center (spectrum 3) than in the sample cut from the wafer edge (spectrum 1), so showing that the vacancy concentration is lower at the wafer edges than in the center as can be expected for the growth conditions of the ingot.^{10,33} Second, the magnitude of the DLTS signal from the thermally activated defect E_1 with its maximum at ~ 110 K is significantly reduced in samples contaminated with nickel when compared to similarly annealed samples without nickel. This suggests that the signal E_1 is due to a vacancy-related defect, as its concentration is reduced when some of the available vacancies are consumed by Nickel. In the wafer center, the concentration of substitutional Ni atoms is found to be close to the solubility limit of nickel in silicon at the temperature of in-diffusion ($[Ni]^{eq} = 1.4 \times 10^{13} \text{ cm}^{-3}$ for $T = 500^\circ\text{C}$).^{22,40} It should be noted, however, that the value given above is the solubility of interstitial Ni in Si at 500°C , which is defined by the equilibrium between the solid solution Si-Ni and NiSi_2 phase on the surface. If there are sinks for interstitial Ni atoms (e.g., vacancies) and there is no equilibrium between interstitial Ni and these sinks, it is possible that the concentration of the introduced Ni atoms in the bulk will exceed the (interstitial) solubility value. So, the $[Ni_s]$ value measured by DLTS can be considered as the lower limit of the vacancy concentration in the N-rich Fz-Si samples.

Nickel diffusion measurements were also carried out on samples of nitrogen lean float zone silicon, in which the carrier lifetime reduction upon annealing is much less severe. The results of DLTS measurements on nitrogen lean silicon with and without evaporated nickel following annealing at 500°C for 90 min are shown in Fig. 9.

In agreement with the data presented in Fig. 4, samples of annealed nitrogen lean float zone silicon with no evaporated nickel (spectra 2 and 4) do not have any deep level

traps with concentration higher than 10^{11} cm^{-3} following annealing at 500°C . In the DLTS spectra of samples with evaporated nickel (spectra 1 and 3), two dominant DLTS signals with their maxima at ~ 45 K and ~ 220 K due to substitutional nickel are present, indicating the presence of vacancies with concentration $\sim (2-3) \times 10^{12} \text{ cm}^{-3}$. Some small peaks with their maxima at ~ 110 K and ~ 190 K appear in the DLTS spectra of the nickel diffused samples N-lean samples. Although positions of these peaks are similar to those of the E_1 and E_2 traps in N-rich samples, it is unlikely that these are due to the same defects, as the small peaks do not appear in samples without nickel contamination. As these samples have been etched in HF:HNO_3 after in-diffusion of nickel, it is possible that these small peaks are related to nickel-hydrogen complexes, similar to those described in Ref. 41. It can also be seen that the concentrations of vacancies at the wafer center (spectrum 3) and edge (spectrum 1) do not differ as much as in nitrogen rich Si. It is likely that a majority of vacancies in the central region of nitrogen lean FZ-Si material have either recombined with self-interstitials or formed some extended defects (voids or clusters) during ingot growth, thereby limiting the number of un-clustered vacancy sites with which interstitial Ni atoms can react.

Crucially, from the magnitudes of the DLTS peaks, we see that the concentration of substitutional nickel and consequently the vacancy concentration are an order of magnitude lower in the nitrogen lean float zone silicon studied in this work than in the nitrogen rich samples. These vacancies could interact with impurities upon annealing and be responsible for the formation of the recombination active defects upon annealing in the temperature range of 450 – 700°C , with greater lifetime degradation occurring in samples with higher vacancy concentration.

IV. DISCUSSION

The work presented in this paper provides further confirmation of the thermally induced minority carrier lifetime reduction presented in Refs. 4 and 6 and demonstrates the formation of a range of deep level defects in nitrogen-rich float zone silicon upon annealing in the temperature range of 450 – 700°C . A summary of the electrically active levels observed in this work and their properties is shown in Table I.

The defects shown to be present in the material studied in this work are different to those found in previous studies of lifetime degradation of float zone silicon,^{4,6} although the annealing procedures were similar. In Ref. 6 for example, four DLTS levels were shown to be present following annealing of n-type FZ silicon for 30 min at 500°C with activation energies for electron emission being 0.16, 0.20, 0.28, and 0.36 eV from the conduction band. Although the levels at $E_c - 0.20$ and $E_c - 0.36$ eV in Ref. 6 are close to the E_1 and E_2 traps presented in this work, a direct comparison of the Arrhenius data used to calculate the activation energies shows that the defects are unlikely to be the same in the two materials. It should be noted that the materials studied in Ref. 6 and in the present work are from different wafer manufacturers. Generalising, we have measured thermally

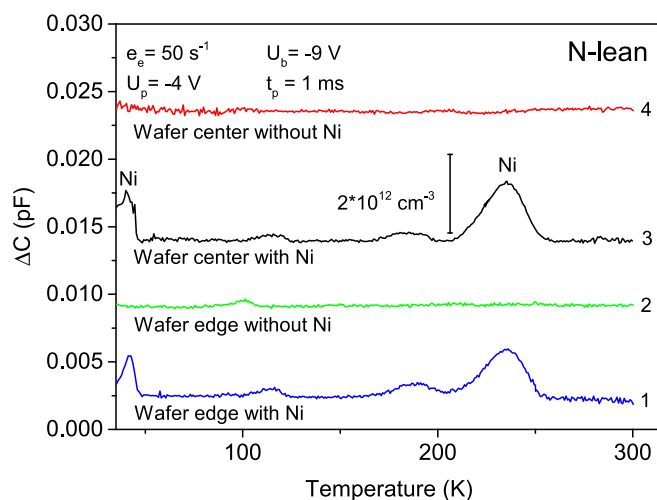


FIG. 9. DLTS spectra recorded on n-type nitrogen lean float zone silicon cut from the wafer edge (spectra 1 and 2) and center (spectra 3 and 4) with (spectra 1 and 3) and without (spectra 2 and 4) thermal evaporation of nickel, following annealing at 500°C for 90 min in N_2 . Measurement settings and the defect concentration unit bar are shown in the graph. The spectra are shifted on the vertical axis for clarity.

induced changes in lifetime and deep level defect spectra in state-of-the-art FZ-Si wafers from a number of manufacturers and found that regardless of the material, lifetime degradation occurred in wafers annealed in the temperature range between 450 and 700 °C.^{3–6} The lifetime changes are more severe in nitrogen rich wafers. However, thermally induced deep level defects in FZ-Si wafers are numerous and their number, parameters, and concentrations depend on: (i) material, (ii) temperature of annealing, and (iii) duration of annealing. It appears that defect reactions, which occur in FZ-Si wafers upon annealing, result in the appearance of deep level defects which depend on the defect-impurity ensemble in the as-grown wafers. Some evidence for the involvement of Si lattice vacancies and nitrogen impurity atoms in the formation of thermally induced deep level defects has been presented.^{3–6} It is possible that oxygen and carbon impurity atoms are also involved in some of the defect reactions. Concentrations of oxygen and carbon impurity atoms are not very high in FZ-Si materials but the values are comparable to (or even higher than) the concentration of intrinsic defects and nitrogen. Identification of the thermally induced deep level defects in FZ-Si wafers is an extremely difficult task. It requires spectroscopic measurements on samples with carefully controlled concentrations of intrinsic defects and nitrogen, oxygen, and carbon impurity atoms.

In this paper, we have studied two float zone materials from the same manufacturer, which were grown under the same conditions except nitrogen content in the growth ambient atmosphere. Wafers from the two crystals were subjected to the same annealing procedures, so allowing the effect of nitrogen incorporation to be isolated. The stark differences shown in this work in both minority carrier lifetime reduction and defect concentration between nitrogen rich and nitrogen lean silicon indicate that nitrogen doping during growth plays an important role in the formation of defect states upon annealing. Our results on samples with the indiffused nickel are consistent with the previous findings that the presence of nitrogen during growth with fast pulling rates suppresses agglomeration of vacancies into large voids and leads to a greater concentration of small vacancy complexes (e.g., the tetravacancy, V_4 , the pentavacancy V_5 or the hexavacancy, V_6). As regards of the V_n complexes with $4 \leq n \leq 6$, in the minimum energy four-fold-coordinated configurations these defects do not have dangling bonds and, so, are expected to be electrically neutral with no levels (and detectable DLTS signals) in the gap (Ref. 42). According to the results of the above-mentioned work, the binding energy of vacancies in the small vacancy complexes is about 2.5 eV. So, the V_n ($4 \leq n \leq 6$) defects can be dissolved at temperatures exceeding 400 °C and releasing vacancies can interact with other defects in Si lattice.^{10,14,15} These results also indicate that the E_1 trap seen in the highest concentration in this work is likely to be due to a vacancy-containing complex. As well as this, we have found that in nitrogen lean silicon samples studied in this work, the concentration of small vacancy complexes is much lower than in similar nitrogen rich samples, consistent with the lifetime measurements where nitrogen lean silicon samples show less degradation when subject to 450–700 °C compared to nitrogen rich Si.

Beyond the differences in concentrations of deep level defects observed in this work in N-rich and N-lean materials, there are some other properties of nitrogen in silicon which suggest it could be a constituent of the deep-level defects seen in this study. First, the annealing characteristics of nitrogen in silicon are similar to those for the defects discussed in this work; in particular, the permanent deactivation of defects as a result of annealing at high temperatures (>900 °C) can be linked with the disappearance of N_2 . The di-interstitial nitrogen defect has been shown in infrared absorption studies^{16,17,43} to display IR absorption lines at 963 and 766 cm^{-1} which are reduced after annealing at temperatures >800 °C due to decomposition or precipitation of N_2 and disappear completely upon annealing at 1100 °C, “where the N-N pair bands anneal out completely.”¹¹ As such, if nitrogen is directly involved in the defect species seen in this work, the permanent deactivation could be due to nitrogen annealing out of the silicon upon heat-treatments at high temperatures,⁴⁴ after which it can no longer interact with other defects forming recombination active complexes.

The majority nitrogen species in silicon (the di-interstitial pair) is thought to be electrically inactive;^{16,19} however, complexes of nitrogen with other impurities and intrinsic defects can introduce electrically active states in the silicon band gap. Nitrogen-oxygen complexes^{7,11,18} have been observed in Czochralski grown silicon to present shallow donor levels, but require significant oxygen concentrations to form and so are unlikely to appear in the material used in this study. A number of complexes of nitrogen with intrinsic defects can also be formed, and several of these are predicted by theory to be electrically active.¹⁹ In a recent paper by Inoue and Kawamura,⁴⁵ nitrogen doped float zone silicon was studied by infrared absorption spectroscopy following electron irradiation and annealing at temperatures between 200 and 800 °C. Infrared absorption lines associated with complexes of nitrogen with vacancies were seen to appear following electron irradiation and were assigned to VN_2 . Upon annealing at temperatures between 200 and 600 °C, a new absorption peak was observed at 689 cm^{-1} and assigned to V_2N_2 , which was seen to removed following annealing at 800 °C. The annealing behaviour of this complex in Ref. 45 is similar to that of the thermally activated defects in float zone silicon presented in Ref. 4.

In addition to its similar annealing behaviour, the V_2N_2 complex of two substitutional nitrogen atoms, N_s-N_s , is predicted to present a level at $E_c-0.2$ eV,¹⁹ close to the most prominent level seen in the nitrogen rich samples in this study (E_1), as well as to experimentally observed nitrogen complexes at $E_c-0.19$ eV^{36,46} with similar electronic properties to the E_1 level. The N_s-N_s structure is predicted to be able to trap further vacancies, which along with smaller structures such as substitutional nitrogen, N_s , and its complexes with vacancies provide numerous electrically active states which could be responsible for the levels seen in this study. Further measurements, using IR spectroscopy could allow identification of the electrically active defects presented in this work; however, a combination of the low concentration of defects and relatively small thicknesses

the wafers used in this study make such measurements unfeasible.

V. SUMMARY

In this work, we have investigated the role of nitrogen in the thermal activation of defects in float zone silicon at temperatures around 500 °C. It has been shown that in silicon containing nitrogen introduced during crystal growth, the reduction in minority carrier lifetime upon annealing, as well as the associated concentration of thermally activated defects, is much higher than in nitrogen lean samples. Both electron and hole traps have been observed in the nitrogen rich material, and the defects have been characterized. We have shown that the introduction of defect states is independent of the annealing ambient atmosphere, providing further evidence that precursors of the thermally activated defects found in this material are introduced during crystal growth, and the defects are activated in the bulk of the material upon annealing.

The significant differences observed between the introduction of defects in nitrogen rich and nitrogen lean materials strongly suggest that nitrogen doping during growth is an important factor in the thermal activation of defect states. In the samples studied in this work, we show that the concentration of un-clustered vacancies is higher than 10^{13} cm^{-3} in nitrogen-doped material and is about $(2\text{--}3) \times 10^{12} \text{ cm}^{-3}$ in nitrogen-lean FZ-Si. These vacancies could then act as a recombination-active defect precursor and form electrically active complexes with other impurities upon annealing. There are some indications that nitrogen atoms are involved in the electrically active defect species introduced upon annealing; however, further experiments are required to find the composition and structure of the thermally activated defects responsible for the lifetime degradation in FZ-Si.

ACKNOWLEDGMENTS

This work has been supported by the EPSRC under the SuperSilicon PV project (EP/M024911/1). The PL imaging set-up was funded by an EPSRC First Grant (EP/J01768X/2). We would like to thank Dr. Ian Hawkins for his support throughout this work, as well as Dr. J. Slotte and Dr. N. Arutyunov for carrying out positron annihilation spectroscopy measurements. The data created during this research are openly available from a data archive at <https://doi.org/10.17632/jgwhkcj6c5.1>.

¹W. Von Ammon, *Phys. Status Solidi A* **211**(11), 2461 (2014).

²E. Golla, *Crystal Growth and Evaluation of Silicon for VLSI and ULSI* (CRS Press, 2014), Chap. 8, pp. 247–282.

³N. E. Grant, F. E. Rougieux, D. MacDonald, J. Bullock, and Y. Wan, *J. Appl. Phys.* **117**, 055711 (2015).

⁴N. E. Grant, V. P. Markevich, J. Mullins, A. R. Peaker, F. Rougieux, and D. Macdonald, *Phys. Status Solidi RRL* **10**(6), 443 (2016).

⁵F. E. Rougieux, N. E. Grant, D. Macdonald, and J. D. Murphy, in *2015 IEEE 42nd Photovoltaic Specialist Conference, PVSC* (2015).

⁶N. E. Grant, V. P. Markevich, J. Mullins, A. R. Peaker, F. Rougieux, D. Macdonald, and J. D. Murphy, *Phys. Status Solidi A* **213**, 2844 (2016).

⁷F. E. Rougieux, N. E. Grant, C. Barugkin, D. MacDonald, and J. D. Murphy, *IEEE J. Photovoltaics* **5**, 495 (2015).

⁸D. Sperber, A. Heilemann, A. Herguth, and G. Hahn, *IEEE J. Photovoltaics* **7**(2), 463 (2017).

⁹T. Niewelt, M. Selinger, N. E. Grant, W. Kwapił, J. D. Murphy, and M. C. Schubert, *J. Appl. Phys.* **121**, 185702 (2017).

¹⁰W. von Ammon, R. Hölzl, J. Virbulis, E. Dornberger, R. Schmolke, and D. Gräaf, *J. Cryst. Growth* **226**, 19 (2001).

¹¹T. Abe, *J. Cryst. Growth* **334**, 4 (2011).

¹²K. Sumino, I. Yonenaga, M. Imai, and T. Abe, *J. Appl. Phys.* **54**, 5016 (1983).

¹³C. R. Alpass, J. D. Murphy, R. J. Falster, and P. R. Wilshaw, *J. Appl. Phys.* **105**, 013519 (2009).

¹⁴H. Kageshima, A. Taguchi, and K. Wada, *Appl. Phys. Lett.* **76**, 3718 (2000).

¹⁵W. Von Ammon, P. Dreier, W. Hensel, U. Lambert, and L. Köster, *Mater. Sci. Eng. B* **36**, 33 (1996).

¹⁶R. Jones, S. Aberg, F. B. Rasmussen, and B. B. Nielsen, *Phys. Rev. Lett.* **72**, 1882 (1994).

¹⁷M. W. Qi, S. S. Tan, B. Zhu, P. X. Cai, W. F. Gu, X. M. Xu, T. S. Shi, D. L. Que, and L. B. Li, *J. Appl. Phys.* **69**, 3775 (1991).

¹⁸V. V. Voronkov, M. Porrini, P. Collareta, M. G. Pretto, and R. Scala, *J. Appl. Phys.* **89**, 4289 (2001).

¹⁹J. Goss, I. Hahn, R. Jones, P. Briddon, and S. Öberg, *Phys. Rev. B* **67**, 045206 (2003).

²⁰L. Dobaczewski, A. R. Peaker, and K. Bonde Nielsen, *J. Appl. Phys.* **96**, 4689 (2004).

²¹R. Brunwin, B. Hamilton, P. Jordan, and A. R. Peaker, *Electron. Lett.* **15**, 349 (1979).

²²M. A. Khorosheva, V. I. Orlov, N. V. Abrosimov, and V. V. Kveder, *J. Exp. Theor. Phys.* **110**, 769 (2010).

²³M. Jacob, P. Pichler, H. Russel, and R. Falster, *J. Appl. Phys.* **82**, 182 (1997).

²⁴O. V. Feklisova and E. B. Yakimov, *Solid State Phenom.* **95–96**, 495 (2004).

²⁵K. Graff, *Metal Impurities in Silicon-Device Fabrication* (Springer-Verlag, Berlin/Heidelberg, 2000).

²⁶L. Scheffler, V. I. Kolkovsky, and J. Weber, *J. Appl. Phys.* **116**, 173704 (2014).

²⁷S. Tanaka, T. Ikari, and H. Kitagawa, *Jpn. J. Appl. Phys., Part 1* **41**, 6305 (2002).

²⁸S. Tanaka and H. Kitagawa, *Physica B* **401–402**, 115 (2007).

²⁹T. Trupke, R. A. Bardos, M. C. Schubert, and W. Warta, *Appl. Phys. Lett.* **89**, 044107 (2006).

³⁰N. E. Grant, T. Niewelt, N. R. Wilson, E. C. Wheeler-Jones, J. Bullock, M. Al-Amin, M. C. Schubert, A. C. van Veen, A. Javey, and J. D. Murphy, *IEEE J. Photovoltaics* **7**, 1574 (2017).

³¹A. I. Pointon, N. E. Grant, E. C. Wheeler-Jones, P. P. Altermatt, and J. D. Murphy, *Sol. Energy Mater. Sol. Cells* **183**, 164 (2018).

³²J. Lindroos, D. P. Fenning, D. J. Backlund, E. Verlage, A. Gorgulla, S. K. Estreicher, H. Savin, and T. Buonassisi, *J. Appl. Phys.* **113**, 204906 (2013).

³³V. V. Voronkov, *J. Cryst. Growth* **59**, 625 (1982).

³⁴V. V. Kveder, Yu. A. Ossipyan, W. Schroeter, and G. Zoth, *Phys. Status Solidi A* **72**, 701 (1982).

³⁵D. Cavalcoli, A. Cavallini, and E. Gombia, *Phys. Rev. B* **56**, 10208 (1997).

³⁶Y. Tokumaru, H. Okushi, T. Masui, and T. Abe, *Jpn. J. Appl. Phys., Part 2* **21**, L443 (1982).

³⁷B. S. Li, C. H. Zhang, Y. R. Zhong, D. N. Wang, L. H. Zhou, Y. T. Yang, L. Q. Zhang, H. H. Zhang, Y. Zhang, and L. H. Hau, *Appl. Surf. Sci.* **257**, 7036 (2011).

³⁸P. K. Giri, S. Dhar, V. N. Kulkarni, and Y. N. Mohaptra, *Nucl. Instrum. Methods Phys. Res. B* **111**, 285 (1996).

³⁹F. Tuomisto and I. Makkonen, *Rev. Mod. Phys.* **85**, 1583 (2013).

⁴⁰E. R. Weber, *Appl. Phys. A* **30**, 1 (1983).

⁴¹M. Shiraisi, J.-U. Sasche, H. Lemke, and J. Weber, *Mater. Sci. Eng. B* **58**, 130 (1999).

⁴²D. V. Makhov and L. J. Lewis, *Phys. Rev. Lett.* **92**, 255504 (2004).

⁴³N. Inoue, T. Sugiyama, Y. Goto, K. Watanabe, H. Seki, and Y. Kawamura, *Phys. Status Solidi C* **13**, 833 (2016).

⁴⁴V. V. Voronkov and R. Falster, *J. Appl. Phys.* **100**, 083511 (2006).

⁴⁵N. Inoue and Y. Kawamura, *J. Appl. Phys.* **123**, 185701 (2018).

⁴⁶K. Nauka, M. S. Goorsky, H. C. Gatos, and J. Lagowski, *Appl. Phys. Lett.* **47**, 1341 (1985).